Mass and charge transport in condensed matter via μSR: localisation and delocalisation.

V G Storchak

Kurchatov Institute, Moscow, Russia

1 Introduction

A vast amount of kinetic processes in chemistry and biology, nuclear and solid state physics, disordered systems and liquids, *etc.* deal with the mass and charge transport, *i.e.* dynamics of neutral (typically atomic) particles and charged particles (typically electrons or electronic complexes), limited by potential barriers. At low temperatures there is no other way to overcome a potential barrier than by quantum tunneling of a particle through it. This phenomenon is called *quantum diffusion* (QD) . The concept of quantum diffusion is introduced for diffusing particles which are heavy compared with electron. On the other hand, a quantum-mechanical evaluation suggests that the tunneling probability is crucially enhanced for light particles. Therefore, in the context of QD the role of the positive *muon* (μ^+) is of particular interest because of its intermediate mass (about 200 times more than that of the electron, but about an order of magnitude less than that of the proton), which is just perfect for the study of QD phenomena. Being a complete chemical analogue of the proton, μ^+ captures an electron and forms the light hydrogen isotope known as *muonium* (Mu = $\mu^+ + e^-$). This happens in insulators and semiconductors, while in metals we deal with the "bare" muon. Because of the unique mass of the muon one can hardly mention any other example where quantum diffusion was observed in such a wide temperature range as for both μ^+ and Mu (for the most recent review see Storchak and Prokof'ev (1998)). The other reason for the success of the quantum diffusion study using muons is the sensitivity of the muon spin relaxation (μSR) and muonium spin relaxation (MSR) techniques (see e.g. Schenck (1986), Cox (1987), Brewer(1995)) to μ^+ and Mu dynamics.

The basic issue in nonclassical transport is whether a wave-like or particle-like description is appropriate, *i.e.* whether the tunneling is coherent or incoherent . This depends on whether the interaction with the environment is such as to lead to spatial localisation of the wave function or to bandlike (Bloch wave) motion. One of the possible channels for

localisation of a particle is through its interaction with lattice excitations (phonons, librons, magnons *etc.*). In a dissipative environment (Caldeira and Legett 1983a, Caldeira and Legett 1983b, Weiss 1993) the lattice excitations can be represented as a bath of harmonic oscillators; interaction with this environment causes a crossover from coherent quantum tunneling to incoherent hopping dynamics when the particle "dressed" with the lattice excitations can be effectively thought of as a polaron.

At low temperatures, the environmental excitations are frozen out. In this case, conventional understanding suggests that the only possible channel for particle localisation is the introduction of crystal disorder, which thus may dramatically change the transport properties of a solid. A well-known example is the spatial localisation of electron states near the Fermi level in a disordered metallic system, which leads to a transition into a dielectric state (the Anderson transition) (Anderson 1958). The concept of Anderson localisation suggests that the wave function of a particle in a random potential may change qualitatively if the randomness becomes large enough. Coherent tunneling of a particle is possible only between levels with the same energy (*e.g.* between equivalent sites); in the case of strong randomness, states with the same energy may be too distant (spatially separated) for tunneling to be effective.

Although the concept of localisation has been introduced primarily in order to describe the electronic transport properties of condensed matter, it may also be applied to the quantum dynamics of heavier particles, whether charged or neutral (Kagan and Prokof'ev 1992, Weiss 1993, Regelmann *et al.* 1995). Recent experimental results for positive muons as well as for muonium atoms clearly indicated that interaction with crystal excitations and crystal disorder dramatically changes the nature of tunneling dynamics for particles about 200 times heavier than the electron.

In condensed matter, the transport of a charged particle depends upon the adiabaticity of its interaction with excitations of the environment. For particles slow enough that electronic excitations are prohibited, the general picture depends critically on the interplay of two characteristic times. The first represents the typical time that a charged particle spends interacting with a given atom or molecule: $\tau_i = a/v$, where a is the lattice constant and v is the velocity of the charged particle. The other characteristic time is ω^{-1}, where $\hbar\omega$ is the characteristic phonon energy. Fast particles ($\omega\tau_i \ll 1$) move through the medium retaining their "bare" identity, whereas charge carriers moving so slowly that $\omega\tau_i > 1$ are followed "instantaneously" by phonon modes and are best thought of as a *polaron* (Holstein 1959) whose mobility is drastically decreased. This crossover from the fast ($\omega\tau_i < 1$) to the slow ($\omega\tau_i > 1$) regime thus leads to a dramatic change in charge transport properties.

In this lecture we discuss recent studies on both quantum diffusion and electron transport in condensed matter using μSR techniques paying particular attention to processes of particle localisation and delocalisation.

2 Quantum diffusion via μSR

The basic concept introduced in order to describe any type of the tunneling dynamics is the concept of a band motion (coherent tunneling) of a particle with a bandwidth Δ determined by the amplitude of particle's resonance transition (Andreev and Lifshitz

1969, Guyer and Zaner 1969). Particle dynamics in perfect crystal at $T = 0$ presents the implest case of a band motion.

At $T \neq 0$, however, tunneling occurs on the background of the coupling with the excitations of the medium. Since Δ is small, this coupling is always relatively strong. Therefore the tunneling kinetics in a solid is a problem of motion in a system with weak quantum correlations and a strong dynamic interaction with medium excitations (Kagan and Prokof'ev 1992). The basic characteristic of the particle interactions with the medium excitations is the frequency, Ω, of phase correlations damping at neighboring equivalent positions of the particle. Even at low temperatures Ω could be as large as Δ; the temperature raise results in an exponential decrease of the coherent tunneling transition (Kagan and Prokof'ev 1992).

The value of Ω being determined by relative fluctuations of the particle interaction with the medium at neighbouring sites only is independent of the amplitude of resonant transition and, subsequently, the value of Δ. Therefore, the transition temperature from band motion to an incoherent tunneling (which involves, for example, absorption or emitting of phonons) is crucially dependent of the particle's mass.

Muonium atom is the ideal choice for a diffusing particle, both by virtue of its light mass and by virtue of the ease with which its mobility can be measured *via* the muon spin relaxation techniques. The importance of μSR techniques to experimental studies of quantum diffusion is illustrated by wide variety of crystals, from metals to insulators, in which both the positive muon (μ^+) and muonium atom show tunneling effects (Storchak and Prokov'ef 1998).

Since Δ is small with respect to all other energy parameters in a solid, quantum diffusion is extremely sensitive to crystal imperfections. Therefore, *localisation* of the particle often takes place at a relatively low defect concentration, in which case the interaction with excitations *enables* quantum diffusion of the particle, measurement of which can thus provide information on crystal disorder.

Until very recently studies of Mu diffusion have focussed on nearly perfect crystals, in which bandlike motion of Mu persists at low temperatures. Crystalline defects have been treated mainly as local traps (Kadono 1992) with trapping radii on the order of the lattice constant a. The justification for such an approach was that the characteristic energy of the crystalline distortion, $U(a)$, is usually much less than the characteristic energy of lattice vibrations, Θ. Unfortunately, since it does not take the particle bandwidth Δ into consideration, this comparison turns out to be irrelevant to the problem of particle dynamics, for which the crucial consideration is that Δ is usually several orders of magnitude less than $U(a)$. For example, a typical Mu bandwidth in insulators is on the order of $\Delta \sim 0.01$–0.1K (Storchak *et al*1994a, Kagan 1990), whereas $U(a)$ could be as large as 10 K. In metals the mismatch is even more drastic: typical values [$U(a) \sim 10^3$K *vs.* $\Delta \sim 10^{-4}$K] differ by about seven orders of magnitude. Under these circumstances, the influence of crystalline defects extends over distances much larger than a. If the "disturbed" regions around defects overlap sufficiently, complete particle localisation can result. An understanding of the possible mechanisms of particle localisation and delocalisation in crystals due to interactions with crystalline defects and lattice excitations is very important in the context of quantum diffusion phenomena.

In this lecture we concentrate our attention on Mu quantum diffusion phenomena in

insulators. A more general review of muon and muonium diffusion in a variety of materials may be found elsewhere (Storchak and Prokof'ev 1998).

2.1 Muonium spin dynamics

The effective spin Hamiltonian of muonium in crystals is usually taken to be of the form

$$\mathcal{H} = hA\,\mathbf{S}_e \cdot \mathbf{S}_\mu - g_e\mu_B \mathbf{S}_e \cdot \mathbf{H} - g_\mu\mu_\mu \mathbf{S}_\mu \cdot \mathbf{H} + h\sum_n \delta\,\mathbf{S}_e \cdot \mathbf{S}_n - \sum_n g_n\mu_n \mathbf{S}_n \cdot \mathbf{H}\,, \quad (1)$$

where A is the muonium hyperfine (HF) frequency, $\mathbf{H}$ is the external magnetic field and the $\mathbf{S}$, g and μ terms are respectively the spins, g-factors and magnetic moments of the various particles. The summations are over all nearby nuclei. The nuclear hyperfine interaction (NHI) between the muonium electron and neighbouring nuclear dipoles is characterised by the frequency δ. The NHI term is represented as isotropic in Equation (1) and so may represent either an average magnetic dipole interaction, in a local field approximation, or a contact interaction, in the event that the muonium electron's wavefunction overlaps with the surrounding nuclei. It is this interaction which sets the timescale for muon spin relaxation.

Qualitatively, modulation of the nuclear hyperfine interactions results in relaxation of the muonium electron spin, which in turn leads to depolarisation of the muon spin *via* the muonium hyperfine interaction.

In transverse field, the relaxation rate T_2^{-1} of the muonium precession signal has a simple form in two limits: if muonium "hops" from site to site at a rate τ_c^{-1} which is much larger than the NHI frequency δ (*fast hopping* limit), then the transverse relaxation rate is given by $T_2^{-1} \approx \delta^2\tau_c$, which is proportional to the effective width of the local field distribution due to nuclear hyperfine interactions, motionally averaged (hence "narrowed") by fast muonium diffusion with $\tau_c^{-1} \gg \delta$. For very *slow* diffusion ($\tau_c^{-1} \lesssim \delta$) muon spin relaxation takes place on a time scale shorter than τ_c and $T_2^{-1} \approx \delta$. (For this reason, the parameter δ is sometimes referred to as the "static width" due to NHI.) Slow muonium dynamics cannot, therefore, be studied by transverse field measurements. Typical example of muonium T_2^{-1} measurements is shown on Figure 1.

The interpretation of longitudinal field (LF) measurements of the muonium spin relaxation rate (T_1^{-1}) is based on the notion that the nuclear hyperfine interactions may be treated as an effective magnetic field acting on the muonium electron. Muonium diffusion causes fluctuations of this effective field which induce transitions between the coupled spin states of the electron and muon. The resultant muon depolarisation is revealed in the forward-backward asymmetry of the muon decay. Such measurements allow values of τ_c^{-1} and δ to be determined independently (Celio 1987). A general expression involves various transitions between the coupled spin states (Cox and Sivia 1994) but a reasonable approximation is obtained by assuming dominance of the lowest frequency transition (within the muonium triplet spin states), leading to the expression

$$T_1^{-1} = \frac{2\delta^2\tau_c}{1+\omega_{\mathrm{Mu}}^2\tau_c^2}\,, \quad (2)$$

where $\omega_{\mathrm{Mu}} = \gamma_{\mathrm{Mu}}H$ is the muonium intra-triplet transition frequency in the magnetic field ($\gamma_{\mathrm{Mu}}/2\pi = 1.4012\mathrm{MHz/G}$). This approach is restricted to the limit of relatively high

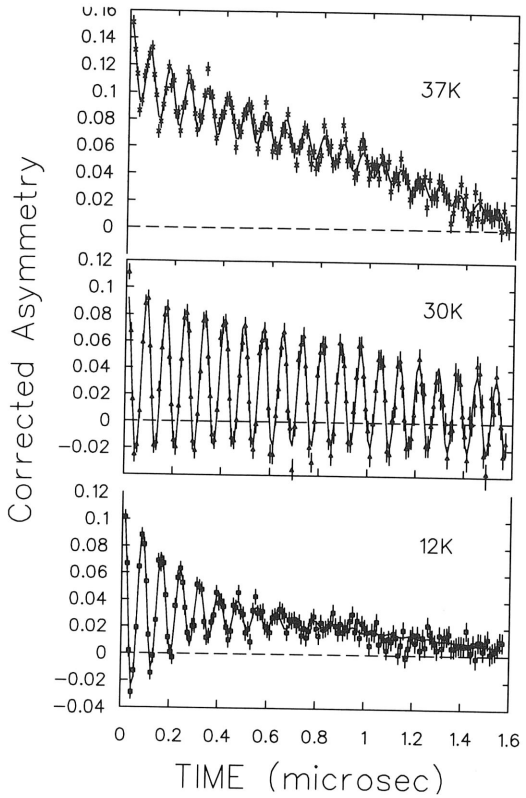

Figure 1. *Muonium precession signals in solid nitrogen in a transverse magnetic field of 8.9G at several temperatures.*

longitudinal fields, however, since the effective magnetic field approximation is valid only if $\gamma_e H \gg \delta$, where γ_e is the electron gyromagnetic ratio. Moreover, in the limit of slow muonium hopping and high magnetic field, T_1^{-1} is generally too low [see Equation (2)] to be measured by the standard μSR technique. Thus high LF measurements, which are very sensitive to muonium dynamics in the fast fluctuation regime, are rather ineffective for the study of very slow dynamics. Figure 2 presents typical example of muonium T_1^{-1} measurements.

Zero field (ZF) and weak longitudinal field (wLF) measurements turn out to be much more sensitive to slow muonium dynamics, at least in the case where the spin response is determined by dipolar interactions with neighbouring nuclei. This is due primarily to the fact that these techniques involve the *full* dipolar Hamiltonian rather than just the *secular* part (as is adequate for the transverse field technique; see, for example, Slichter (1980)). A classical treatment (Kubo and Toyabe 1966) gives an analytical expression for the time evolution of the muon polarisation function in zero field, known as the Kubo-Toyabe function: for a Gaussian distribution of static local fields, with second moment proportional to Δ^2,

$$P(t) = \frac{1}{3} + \frac{2}{3}\left(1 - \Delta^2 t^2\right) \exp\left(-\frac{1}{2}\Delta^2 t^2\right) . \qquad (3)$$

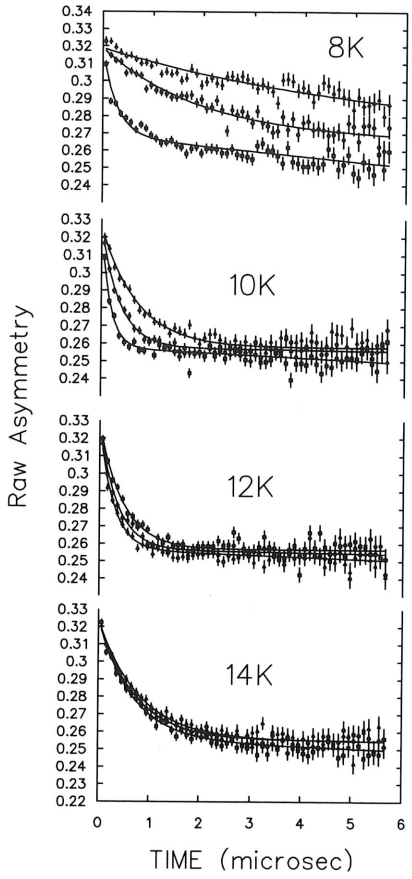

Figure 2. *μSR spectra in longitudinal field in solid nitrogen for $B_{\|} = 4G$ (triangles), 8G (circles) and 12G (squares) at different temperatures.*

An important feature of Equation (3) is the "1/3 tail" which, roughly stated, reflects the fact that 1/3 of the muon polarisation is, on average, aligned parallel to the local field while 2/3 is transverse to the local field and thus precesses. Although this function was first adopted and experimentally confirmed for μ^+ spin relaxation Hayano *et al.* (1979), it is equally applicable for the triplet state of muonium, which can be treated in low magnetic field as one particle with spin $S = 1$. Figure 3 presents the first and as far as the author knows the unique observation of the Kubo-Toyabe relaxation function for the muonium atom. Very slow diffusion, in which the muonium atom jumps between sites with uncorrelated arrangements of neighbouring nuclear spins, is manifest in an observable relaxation of this "1/3 tail" (Kubo and Toyabe 1966, Hayano *et al.* 1979). A "strong-collision" treatment (Kubo 1954, Hayano *et al.* 1979) gives a relaxation function in this regime which may be written (for times $t \gg \Delta^{-1}$) as

$$P(t) \approx \frac{1}{3} \exp\left(-\frac{2}{3}\frac{t}{\tau_c}\right) . \tag{4}$$

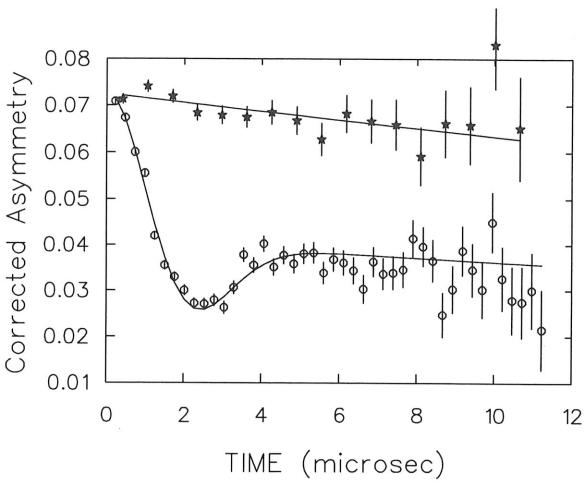

Figure 3. *Time dependence of the muonium polarisation in solid Kr at $T = 20.3K$ in zero magnetic field (circles) and in a weak longitudinal magnetic field $B = 5G$ (stars). Note the Kubo-Toyabe form of the muon polarisation function in zero magnetic field.*

This expression for $P(t)$, being independent of Δ, may be used for *direct* measurements of very slow muonium hop rates.

In weak longitudinal field the "tail" of the relaxation function which is sensitive to slow dynamics is shifted to earlier times and has an amplitude several times higher than the "1/3 tail" of the zero field function (Luke *et al.* 1991). This makes the wLF technique even more sensitive than ZF for measurements of extremely slow muonium hop rates. An example of muonium spin relaxation spectra in weak longitudinal field is shown in Figure 4.

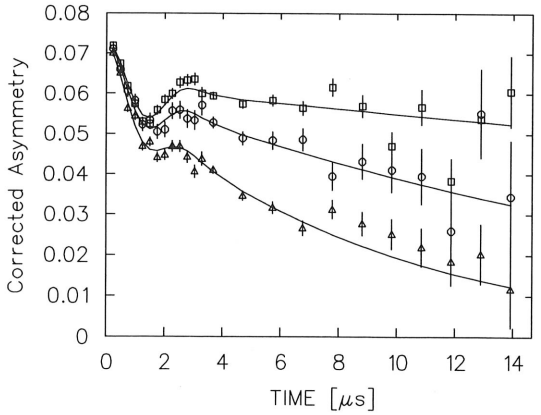

Figure 4. *Muonium polarisation time spectra in solid Kr in a very weak longitudinal magnetic field $B = 0.22G$ at different temperatures: 25K (squares), 28K (circles) and 30K (triangles).*

2.2 Muonium localisation in the one-phonon QD regime

The tunneling motion of a particle in a solid is often governed by two channels of the interaction with the medium. The first channel gives rise to the effect of fluctuational preparation of the barrier (FPB) (Kagan and Klinger 1976) and characterises the interaction of a particle with barrier fluctuations during the passage through the barrier region. The second channel is due to intrawell interaction and manifests the appearance of the polaron effect (PE) (Flynn and Stoneham 1970).

As long as the diffusing particle is much lighter than the atoms composing the medium, the former will vibrate at a characteristic frequency ν_0 much higher than the typical vibrational frequency of the latter, which is of the order of the crystal's Debye temperature Θ. In this case a light interstitial atom will respond almost adiabatically to lattice vibrations, including the quantum zero-point motion (ZPM) of nearby lattice atoms, resulting in an enhanced tunneling probability when the surrounding atoms happen to assume a configuration in which the barrier along the optimal particle path separating the current interstitial site from a neighbouring one is instantaneously lower and/or narrower than on average. This version of FPB applies even at zero temperature and increases the rigid-lattice tunneling bandwidth Δ_0 of the particle to an effective $T = 0$ bandwidth $\Delta = \Delta_0 e^G$ in the absence of other effects (see below). The FPB exponent G is proportional to the mean square fluctuations of the quasiclassical tunneling action and can be expressed conveniently as $G \sim (\delta U_B/\hbar\nu_0)^2$, where δU_B is a typical fluctuation of the barrier height.

The observed value for the bandwidth is also renormalised because of the PE which inevitably occurs in any non-rigid lattice: the interstitial atom causes the surrounding lattice to relax slightly, "digging a hole" for itself and lowering its energy in the current site by E_P relative to that which one would calculate for a perfectly rigid lattice. The combination of self-trapped interstitial and accompanying lattice distortion are commonly referred to as a quasiparticle known as a *small polaron*. The effect of the PE energy shift E_P is to decrease the probability of resonance between the energy of the light atom in its current interstitial site and the energy it would have in an adjacent site prior to reconfiguration of the lattice distortion. In effect, this *narrows* the tunneling bandwidth, giving $\Delta = \Delta_0 e^{-\phi} e^G$ at $T = 0$, where ϕ is another dimensionless parameter describing the reduction of resonant tunneling opportunities due to the PE energy shift. Actually the particle has to wait for the lattice fluctuation which brings the distorted configuration around the initial particle site into the symmetric configuration allowing resonant transition between the sites. Such a fluctuation is very rare if adjacent atoms' displacements δu are large compared with the root mean square ZPM amplitude $\sqrt{\langle u^2 \rangle_0}$. One can estimate the polaron factor in the exponent as $\phi \sim \delta u^2/\langle u^2 \rangle_0 \sim E_P/\Theta$.

The parameters ϕ and G are related to the displacements of different groups of atoms, so that one might easily imagine cases when $\delta U_B \gg E_P$—for instance, if the interaction between the particle and a lattice atom is a strong function of the distance between them and the tunneling process leads to their approach. To be more precise, PE and FPB are not completely independent: the PE lattice distortion also alters the average shape and height of the barrier so that, even in the absence of lattice ZPM, there would be a PE-induced renormalisation of the tunneling bandwidth which we may characterise by a separate temperature-independent dimensionless parameter B, giving a final expression

for the tunneling bandwidth (Kagan and Klinger 1976)

$$\Delta = \left(\Delta_0 e^B\right) e^{-\phi} e^G \,. \tag{5}$$

Obviously one can at best measure Δ itself, so it is only through theoretical estimates that one can form opinions about the relative importance of ϕ, which decreases the tunneling rate, G, which increases it, and B, which could do either. At present we are not aware of any first-principles calculations of Δ_0 which are precise enough even to determine the overall sign of $(\Delta - \Delta_0)/\Delta$.

At finite temperatures, real phonons begin to affect the tunneling process. However, in the temperature range $T \ll \Theta$, where the average amplitude of lattice vibrations is hardly changed compared to that due to ZPM, one can describe the particle dynamics in the framework of standard kinetic equations assuming a constant value for the tunneling matrix element (Andreev and Lifshitz 1969). The remarkable phenomenon of crossover from coherent band motion to incoherent hopping (Kagan and Prokof'ev 1992, Storchak *et al.* 1994) takes place in this temperature range where Δ is essentially unchanged. Only at very high temperatures $T \sim \Theta$ do the effective vibrational amplitudes of individual lattice atoms begin to have RMS values significantly larger than those attributable to ZPM, at which point the effects due to FPB acquire temperature dependences.

The PE, which is likely to have a larger effect on the coherent bandwidth at $T = 0$, should become less important at high T (see below), whereas FPB effects increase and become dominant for $T > \Theta$. The mean square vibration amplitude increases linearly with T at high temperature ($\langle u^2 \rangle \approx \langle u^2 \rangle_0 \, T/\Theta$) and so does the mean square fluctuation of the barrier height. Clearly, as the temperature increases so does the probability of "easy" tunneling opportunities as lattice atoms fluctuate away from the particle trajectory connecting adjacent sites. Thus we find $G(T) \approx G(0)\, T/\Theta$. On the other hand, large amplitude vibrations simply wash out the effect of lattice distortion around the particle because all lattice configurations are equally accessible at high T. Substituting $\langle u^2 \rangle_0 \to \langle u^2 \rangle$ in the earlier expression for the polaron exponent, we arrive at the well known result that "polaron narrowing" disappears as $\exp(-E_P/4T)$ (Flynn and Stoneham 1970).

The full expression (including all PE and FPB effects) for the tunneling hop rate τ_c^{-1} is thus (Kagan and Prokof'ev 1992, Kagan and Prokof'ev 1990)

$$\tau_c^{-1} \;=\; \frac{2(\Delta_0 e^B)^2 \sqrt{\pi}}{\sqrt{(E+\gamma)T}} \, \exp\left[-\frac{E}{T} + \frac{T}{E_B} - \frac{T\xi_B^2}{16(E+\gamma)}\right] . \tag{6}$$

where the "activation" energy E is directly related to the polaron shift ($E = E_P/4$) and E_B can be approximated by $E_B \sim \Theta/G(0)$. The last term in the exponent describes a mixing of the two effects because, as mentioned above, in the presence of lattice distortions the average barrier does not correspond to the rigid lattice value. The last two terms in Equation (6) have exactly the same linear temperature dependence and are therefore experimentally indistinguishable; nevertheless, specific choice of the medium under investigation may allow one to separate FPB and PE using Equation (6).

The PE is sure to be much weaker in insulators than the electronic version in metals (Kondo 1984b,Yamada 1984), which can lead to complete localisation of the tunneling particle in a crystal despite translational symmetry. The FPB effect, on the other hand, may become dominant for the case of phonon-coupled neutral atoms in insulators,

whereas FPB is less significant for electron-coupled charged particles in metals (Kagan and Prokof'ev 1992).

The conditions under which one can experimentally separate the effects of FPB from PE are therefore rather specific: One should study a light neutral atom diffusing in a "soft" insulating crystal composed of heavy atoms, ensuring $\nu_0 \gg \Theta$ and minimising any competing PE. One should study the temperature dependence of the tunneling rate τ_c^{-1} at high temperatures $T > \Theta$, where the thermal FPB effect is strongest. One must not, however, approach the temperature $T^* \sim \nu_0$ at which classical over-barrier hopping sets in (Lifshitz and Kagan 1972a, Lifshitz and Kagan 1972b). The region $\Theta < T < T^*$ is most sensitive to one-phonon quantum diffusion (Kagan and Prokof'ev 1992) and will be most likely to reveal FPB effects. This emphasises the need for a medium with a low Debye temperature, *e.g.* a Van der Waals crystal such as solid xenon and krypton, the heaviest solids in which the ideal light interstitial atom for such a study — muonium — has ever been observed (Kiefl *et al.* 1981, Storchak *et al.* 1992a, Storchak, Brewer and Morris 1994a, Storchak *et al.* 1996).

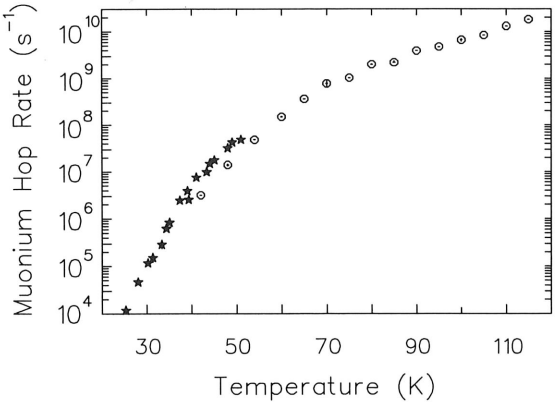

Figure 5. *Temperature dependences of the muonium hop rate in solid Kr (stars) and solid Xe (circles).*

Figure 5 presents the temperature dependences of the muonium hop rates in solid xenon and krypton. First one may notice the six orders of magnitude variation of the muonium hop rates. In solid krypton, the use of both zero field and weak longitudinal field techniques allowed the determination of the slowest Mu hop rates ever measured for μ^+ or Mu. At low temperatures muonium τ_c^{-1} is two orders of magnitude slower than the inverse μ^+ lifetime, the tunneling regime previously inaccessible. In contrast, in solid xenon at high temperatures muonium atom undergoes about 10^4 hops during the μ^+ lifetime, which presents one of the fastest tunneling processes ever measured for μ^+ or Mu. An unprecedented variation of the muonium hop rate over 4 decades in both crystals allowed a direct comparison with the theory using Equation (6). The analysis showed that both PE and FPB effect should be taken into account (Storchak, Brewer and Morris 1994a, Storchak *et al.* 1996). At low temperatures, strong polaron effect causes gradual localisation of muonium atom in heavy rare gas solids.

2.3 Muonium localisation in the two-phonon QD regime

Studies of the diffusion of hydrogen atoms (Steinbinder *et al.* 1988) and μ^+ in metals, as well as Mu diffusion in insulators and semiconductors (Storchak and Prokof'ev 1998) have convincingly shown the quantum mechanical character of the phenomenon, most clearly seen at low temperatures where the particle hop rate τ_c^{-1} *increases* with *decreasing* temperature T according to the power law $\tau_c^{-1} \propto T^{-\alpha}$, thus manifesting the onset of the coherent process. In metals, coupling to conduction electrons is the dominant scattering mechanism (Kondo 1984b,Yamada 1984) and causes $\alpha < 1$. In insulators, where phonon scattering processes prevail, α is predicted (Andreev and Lifshitz 1969, Kagan and Prokof'ev 1992) to be 7 or 9 at low temperatures where the absorption of single phonons shifts the energy of the diffusing particle too much for tunneling to occur and so two-phonon diagrams (which can leave the energy almost unchanged) are expected to dominate. Surprisingly, the experimental results on Mu diffusion in *ionic* insulators (Kadnona 1990) indicate that α is generally close to 3; this "universal" power-law behaviour with $\alpha \approx 3$ prompted Stamp and Zhang (1991) to conclude that muonium diffusion is governed by *one*-phonon scattering. On the other hand, in Kagan and Prokof'ev (1990) it was shown that $\alpha \approx 3$ can also be obtained from *two*-phonon scattering processes if the actual phonon spectrum of the ionic crystal is taken into account; unfortunately, that procedure requires the introduction of adjustable parameters. This basic problem of the validity of the former or the latter remained open until recent results on Mu quantum diffusion in solid nitrogen, methanes and carbon dioxide presented direct experimental evidence of the dominance of two-phonon scattering mechanism in insulators at low temperatures.

Figure 6 and 7 present the results of transverse field measurements in solid nitrogen and methane isotopes, respectively. These crystals show similar non-monotonic temperature

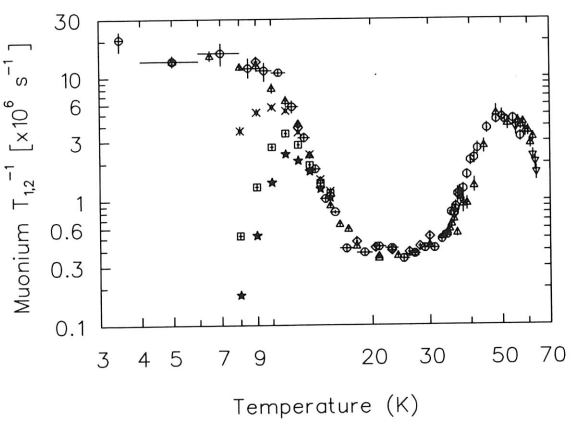

Figure 6. *Muonium relaxation rates in ultra high purity solid N_2 in weak transverse field [circles, triangles, diamonds and inverted triangles correspond to different samples] and several longitudinal fields [stars: 12G; squares: 8G; crosses: 4G].*

dependences of muonium relaxation rate T_2^{-1}. In order to describe the particle's dynamics in these crystals we will follow the experimental results and the analysis of Mu relaxation

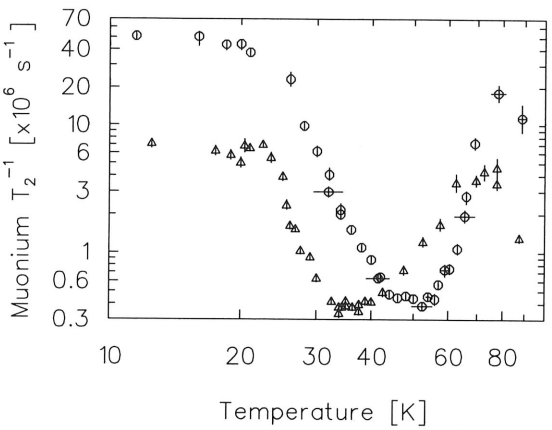

Figure 7. *Temperature dependences of muonium relaxation rate in solid methanes in weak transverse field $H = 5G$ (circles: CH_4; triangles: CD_4).*

in solid nitrogen where muonium QD has been studied in detail (Storchak *et al.* 1993, (Storchak *et al.* 1994, Storchak, Brewer and Morris 1996a, Storchak, Brewer and Morris 1996b.

At low temperatures T_2^{-1} levels off as it is expected for very slow diffusion ($\tau_c^{-1} \lesssim \delta$) regime giving value of NHI frequency $\delta = T_2^{-1}$. Therefore, T_1^{-1} measurements were done to study slow Mu hop rates regime. In longitudinal fields the observed relaxation is attributed entirely to the muonium fraction, as the diamagnetic complex in solid nitrogen is known (Storchak *et al.* 1992b) to be the static $N_2\mu^+$ ion, whose relaxation rate is about 0.1×10^6 s^{-1} — far slower than was observed in experiment. Other possible relaxation mechanisms were also ruled out (Storchak *et al.* 1994).

Figure 6 shows the temperature dependence of T_1^{-1} for several values of longitudinal field along with the results of transverse field measurements in pure solid nitrogen. At temperatures above 15K, where $\omega_0\tau_c \ll 1$, T_1^{-1} becomes independent of field and equal to T_2^{-1}. From Equation (2) we get the well-known (Slichter 1980) relation for fast diffusion ($\delta\tau_c \ll 1$) and low field ($\omega_0\tau_c \ll 1$):

$$T_1^{-1} = 2\delta^2\tau_c = T_2^{-1}. \tag{7}$$

The T_1^{-1}-maximum effect (in NMR known as T_1-minimum effect (Slichter 1980)) is clearly seen around 10–11K for all longitudinal fields. The T_1^{-1}-maximum condition at $\omega_0\tau_c = 1$

$$T_1^{-1}(\max) = \delta^2/\omega_0\ . \tag{8}$$

allows unambiguous determination of NFI frequency and produces an absolute calibration of the Mu hop rate.

Figure 8 presents the temperature dependence of the muonium hop rate τ_c^{-1} in pure solid nitrogen derived from Equation (2) and complemented by the transverse field data for $T > 12$K, where motional narrowing leads to Equation (7).

For temperatures $T \ll \Theta$ (the Debye temperature) quantum diffusion is believed (see

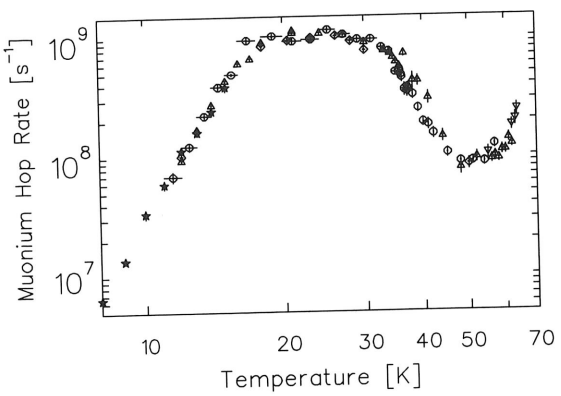

Figure 8. *Temperature dependence of the muonium hop rate in ultra high purity solid N_2. Stars correspond to the combined longitudinal field measurements; other symbols correspond to transverse field measurements in different samples.*

Kagan and Prkof'ev 1992) to be governed by two-phonon processes, for which τ_c^{-1} is

$$\tau_c^{-1} \sim \frac{\tilde{\Delta}_0^2 \Omega(T)}{\Omega^2(T) + \xi^2}, \tag{9}$$

where $\tilde{\Delta}_0$ is the renormalised bandwidth for Mu diffusion and ξ is the typical difference between energy levels of the particle at adjacent tunneling sites due to static disorder.

The main feature of Equation (9) is the minimum of $\tau_c(T)$ at $\xi \sim \Omega(T)$.

$$\text{When } \xi < \Omega, \qquad \tau_c^{-1} \propto \frac{\tilde{\Delta}_0^2}{\Omega(T)}; \tag{10}$$

$$\text{but if } \xi \gg \Omega, \quad \text{then} \quad \tau_c^{-1} \propto \frac{\tilde{\Delta}_0^2 \Omega(T)}{\xi^2}, \tag{11}$$

giving the opposite temperature dependence so that Mu atoms are localised as $T \to 0$. The only effect of the one-phonon interaction at low temperatures is believed to be an exponential renormalisation of the tunneling amplitude (Kagan and Prokof'ev 1992). The two-phonon width $\Omega(T)$ is determined by the phonon spectrum of the lattice. In the $T \to 0$ limit only acoustic phonons are important and

$$\Omega(T) \propto T^{7(+2)}. \tag{12}$$

The two additional powers of T appear only in the case of muonium tunneling between absolutely equivalent sites.

In the temperature range $30 < T < 50$K, the measured Mu hop rate in solid nitrogen exhibits an empirical temperature dependence $\tau_c^{-1} \propto T^{-\alpha}$ with $\alpha = 7.3(2)$; since, from Equation (10), $\tau_c^{-1} \propto \Omega^{-1}(T)$, we have $\Omega(T) \propto T^7$ as expected [Equation (12)]. This is the first experimental confirmation of the T^{-7} dependence of τ_c^{-1} predicted by the two-phonon theory of quantum diffusion (Kagan and Prokof'ev 1992).

Below about 30K the Mu hop rate levels off, presumably due to band motion with an estimated (Storchak *et al.* 1994, Storchak *et al.* 1993) renormalised bandwidth of $\tilde{\Delta}_0 \sim$

10^{-2}K, in agreement with the value deduced from the high-temperature data where one-phonon interactions lead to an enhanced fluctuational preparation of the barrier (FPB) effect (Storchak *et al.* 1993). This value for the Mu bandwidth in solid nitrogen should be compared with the bandwidth scale $\Delta \sim 10^{-4}$K obtained for the quantum diffusion of ^{3}He atoms in ^{4}He crystals (Richards *et al,* 1976). Although the former is much larger, the qualitative similarity of these results suggests a common dynamical behaviour for light particles in insulators, as opposed to metals, where different scattering mechanisms lead to quite different impurity dynamics.

Muonium motion in solid nitrogen slows down again below about 18K, probably due to the orientational ordering of N_2 molecules. For $T < 18$K the data in Figure 8 obey

$$\tau_c^{-1} = \tau_0^{-1} \left(\frac{T}{\Theta}\right)^{\alpha}, \tag{13}$$

with $\Theta = 83$K (Verkin and Prikhotko 1983), $\tau_0^{-1} = 3.6(8) \times 10^{13}\text{s}^{-1}$ and $\alpha = 6.7(1)$.

The change in the temperature dependence of the Mu hop rate from a T^7 to a T^{-7} law reflects a crossover from Equation (10) to Equation (11). Preliminary analysis show that Mu diffusion in solid methane isotopes exhibits similar temperature dependences of τ_c^{-1}. In all three crystals, at low temperatures gradual Mu localisation takes place which reflects a suppression of band motion by static disorder introduced by orientational defects. In solid nitrogen, subsequent reduction of temperature below 10K leads to an inhomogeneous quantum diffusion phenomena.

2.4 Muonium localisation in inhomogeneous QD regimes

Most previous experiments on muonium diffusion have focussed on very pure insulators, in which Mu band motion persists at lowest temperatures and any effects of crystal imperfections are difficult to observe. The static disorder had no chance to dominate Mu diffusion since at low temperatures the muonium bandwidth was larger than ξ, while at higher temperatures Ω increasingly exceeded both ξ and Δ, resulting in the dynamical destruction of the band.

Experimental evidence for Mu localisation in imperfect crystal due to suppression of band motion by static disorder was first observed in a solid nitrogen crystal (Storchak *et al.* 1994). At temperatures well below $T_{\min}$, where $T_{\min}$ is determined by the interplay between $\Omega(T)$ and ξ, the observed transverse field relaxation rate T_2^{-1} of muonium should mainly represent *quasi-localised* Mu atoms in the vicinity of defects. Another fraction of Mu atoms initially located far from impurities or defects should move more rapidly and therefore its muon spin polarisation should relax more slowly in transverse field due to motional narrowing. The crucial point is that at low temperatures inelastic scattering by phonons is strongly suppressed and these two Mu fractions remain distinct (Kagan and Prokof'ev 1992, Prokof'ev 1994). A distinctive two-component composition of the muon polarisation function $P(t)$ is a direct manifestation of the crystal's *spatial inhomogeneity* and must be a universal feature of particle diffusion in imperfect crystals whenever static level shifts ξ exceed $\Omega(T)$.

Of course, the formation of two independent ensembles of particles holds only at very low temperatures where inelastic interactions with the thermal excitations are weak enough. The temperature increase continuously changes the ratio between moving and

localised components. To be more precise, the temperature dependence of τ_c^{-1} is now determined by the interplay between Ω and $\xi(r)$, where r is the distance to the defect. Moreover, one finds that a description of the relaxation function in terms of exponential damping (a "single τ_c" approximation, see, for example, Equation(2)) is no longer valid and crystal inhomogeneity causes a spatial distribution of τ_c^{-1} which we will characterise as $\tau_c^{-1}(r)$. This fact was unambiguously confirmed experimentally for Mu diffusion in solid nitrogen (Storchak *et al.* 1995, Storchak, Brewer and Morris 1999a). A similar feature for μ^+ diffusion in metals was found in (Karlsson *et al.* 1995).

Inhomogeneous muonium QD in solid N_2 has been detected in weak LF experiments at low temperatures. At temperatures above about 10K, excellent fits to the data were obtained using expression (2), which assumes that *all* Mu atoms diffuse at the same rate. However, below 10K the polarisation function clearly consists of two exponential terms (see Figure 9) and it was impossible to fit experimental spectra using a single exponential relaxation function (2). Therefore, experimental time spectra were compared with the simplest possible two-component expression

$$A(t) = A_F \exp(-T_{1_F}^{-1} t) + A_S \exp(-T_{1_S}^{-1} t), \tag{14}$$

where A_F and A_S are the asymmetries (amplitudes) of the fast- and slow-relaxing components and $T_{1_F}^{-1}$ and $T_{1_S}^{-1}$ are their respective relaxation rates.

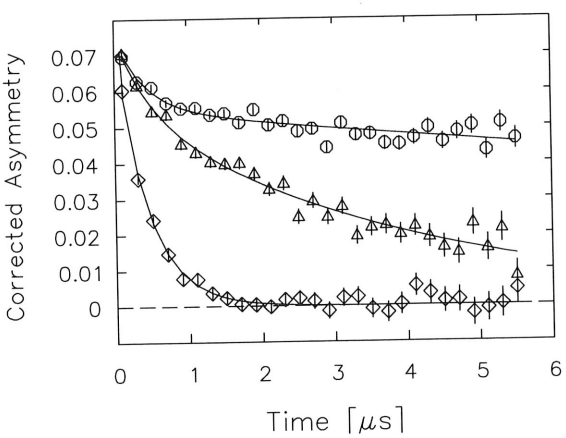

Figure 9. *Muon spin relaxation spectra of Mu in solid nitrogen in longitudinal field $H = 8G$ at $T = 10K$ (diamonds), 8K (triangles) and 6K (circles). Note the presence of two components in the relaxation function at low temperatures.*

Figure 10 shows the temperature dependences of these asymmetries (a) and relaxation rates (b) obtained by fitting expression (14) to the data. Figure 10(c) displays the temperature dependences of the Mu hop rates for the fast and slow components derived from expression (2). Above about 9K, Mu exhibits quantum tunneling with a characteristic $\tau_c^{-1} \propto T^7$ temperature dependence (Storchak *et al.* 1994). Below this temperature the slow component displays strong localisation while the fast component shows temperature-independent Mu motion with about two jumps per muon lifetime.

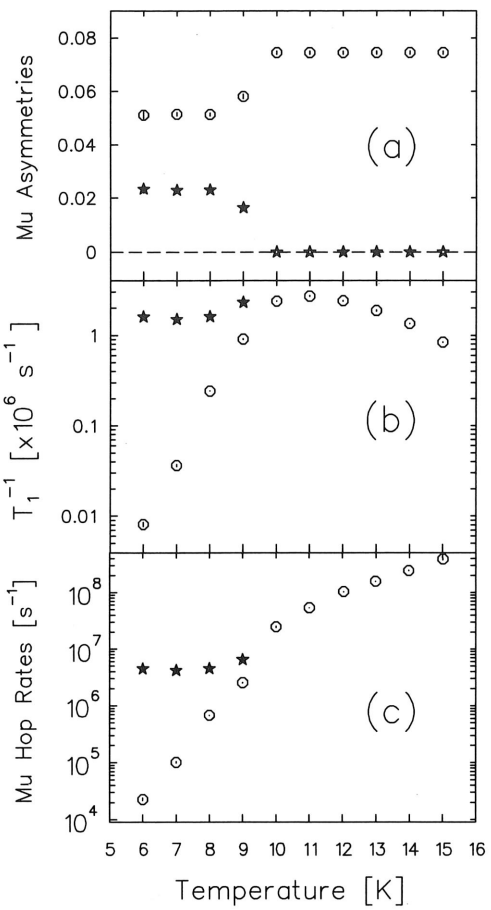

Figure 10. *Temperature dependences of slow-relaxing (circles) and fast-relaxing (stars) muonium signals in solid nitrogen:*
(a) slow (A_S) and fast (A_F) muonium asymmetries (amplitudes);
(b) slow (T_{1S}^{-1}) and fast (T_{1F}^{-1}) longitudinal relaxation rates;
(c) slow (τ_{cS}^{-1}) and fast (τ_{cF}^{-1}) muonium hop rates.

2.5 Localisation via trapping

At low temperatures, even weak interaction with defects may be larger than T leading to effective traps for diffusing particles. As a result, for many years μ^+ and Mu QD in crystals was discussed in terms of trapping effects regardless of the temperature range or the nature of the crystal (see, e.g., Kadono (1990) and references therein). Below we present an experimental evidence that such trapping effects, which may be dominant in metals, are in fact rather ineffective in insulators at low temperatures.

The trapping rate K in an imperfect crystal is given as follows

$$K = 4\pi c n R_T D(R_T), \tag{15}$$

where $c \sim 1$ is a numerical coefficient, n is the impurity concentration, R_T is the trapping radius defined by the condition $U(R_T) = T$ and $D(R_T)$ is the diffusion coefficient (Waite 1957). As for elastic interaction $U = U(a)(a/R)^3$ one could immediately notice that the defect potential has rather *long-ranged* character with $R_T \gg a$. In "dirty" insulators at low temperatures the temperature dependence of $D(R_T)$ is opposite to that in a perfect crystal [see Equations (10) and (11)]. Thus the trapping rate decreases rapidly with temperature, making the trapping mechanism essentially ineffective. This was unambiguously demonstrated in the experiment on Mu diffusion in solid nitrogen doped with 10^{-3} CO impurities (Storchak, Brewer and Morris (1996a).

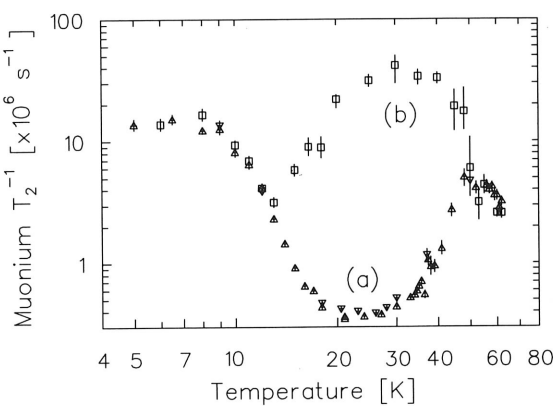

Figure 11. *Temperature dependences of the transverse relaxation rate (T_2^{-1}) of muonium, (a) in pure nitrogen crystals (triangles, two different samples) and (b) in a crystal of N_2+10^{-3} CO.*

Figure 11 shows the temperature dependence of the muonium transverse relaxation rate T_2^{-1} in pure solid N_2 (a, triangles: two samples) and in N_2 with 10^{-3} CO impurities (b, squares). When the Mu atom hops rapidly (causing low values of T_2^{-1} due to dynamical "narrowing"), it finds a CO impurity in the N_2+CO crystal and reacts chemically. This chemical reaction is manifest in an exponential relaxation of the Mu polarisation, the rate of which is determined by the time required for Mu to approach the CO impurity within a distance a, after which the reaction occurs immediately. This description in terms of a chemical reaction controlled by Mu diffusion is perfectly analogous to the phenomenology used to describe trapping.

At high temperatures the clear maximum in T_2^{-1} for Mu in N_2+CO marks the crossover from fast to slow Mu diffusion near CO impurities, which in turn reflects the interplay between $\Omega(T)$ and ξ in the denominator of Equation (9). In this temperature range the strong coupling to phonons allows Mu to overcome the defect potential and move to react with CO.

At low temperatures the suppression of inelastic interactions with the lattice changes Mu diffusion drastically—Mu atoms are stuck (or "frozen") at some distance far from CO impurities, causing a strong reduction of the reaction rate (Mu relaxation rate). Muonium atoms are then effectively excluded from the volumes around the impurities and thus T_2^{-1} is the same as for pure N_2 and N_2+10^{-3}CO crystals, as clearly seen in

the experiment. Similar behaviour of muonium T_2^{-1} was found in CO_2+$10^{-3}N_2O$ system (Storchak, Eschenko, Brewer, *et al.* (unpublished)). Thus muonium localisation *via* trapping is shown to be essentially ineffective at low temperatures in insulators.

3 Electron transport via μSR

Ionisation of matter by high energy charged particle radiation inevitably produces excess electrons and thus may cause electrical breakdown even in wide-gap insulating materials subjected to high electric field. These materials are used in a large number of applications ranging from power generation equipment to micro-electronic devices. It is therefore important to understand the transport mechanisms of radiolysis electrons in insulators. Fast electrons liberated by ionising particles are slowed down by creating secondary electron-ion pairs and excitations of the medium. While extensive knowledge has already been accumulated on electron transport and energy transfer processes at high energy, very little is known about the transport of electrons liberated near the end of the ionisation track. The most natural description of the electron dynamics in this energy domain is in terms of quasi-free states of the electrons interacting with molecular and lattice vibrations. In many cases, rather high mobility allows electrons to be transported over relatively large distances and initiate various observable effects that depend on the transport properties of the host material.

In different insulators, electron transport is determined by qualitatively different interactions of electrons with the medium. Measurements on Ar, Kr and Xe crystals (Miller *et al.* 1968) show clearly that electron mobilities in these solids are comparable to those found in wide-band semiconductors ($b_e \sim 10^3 \mathrm{cm}^2\,\mathrm{s}^{-1}\,\mathrm{V}^{-1}$), which encouraged different authors to apply Shockley's well-known theory (Schockley 1951). An approximation in which the free charge carriers are completely delocalised and the electron-phonon interaction is treated as a perturbation gave an adequate description of the observed electron transport.

The rather low electron mobilities found in the diatomic solids of N_2, CO and O_2 (Loveland *et al.* 1972b) ($b_e \sim 10^{-2}$–$10^{-3}\mathrm{cm}^2\,\mathrm{s}^{-1}\mathrm{V}^{-1}$) suggest that a fundamentally different mechanism of electron transport occurs in these materials. The *localisation* of excess electrons with the formation of a small polaron (Holstein 1959) due to strong interactions with excitations of the medium was proposed to explain such low values of drift mobility.

Measurements of electron mobility by time-of-flight (TOF) technique represent a very direct approach to the study of charge transport properties in solids. It should be noted, however, that in such experiments the path length between electrodes is *macroscopic* ($\sim 10^{-2}$–10^{-1}cm), making the results highly susceptible to spurious TOF changes if electrons interact with crystalline defects such as impurities, strains, and micro-cracks. The muon spin rotation technique avoids these difficulties inherent to the traditional TOF technique because the distances involved are much shorter ($\sim 10^{-6}$–10^{-4}cm).

In μSR experiments each incoming several-MeV μ^+ leaves behind an ionisation track of liberated electrons and ions. Although this circumstance has been disregarded in a great majority of experimental and theoretical studies of condensed matter by μSR techniques, the liberation of electrons by muon radiolysis is far from a negligible effect — in fact, in some insulators and semiconductors it may determine much of the subsequent behaviour

of the system. Recent μSR experiments in liquid helium (Krasnoperov *et al.* 1992), solid nitrogen (Storchak, Brewer and Morris, 1994b), (Storchak, Brewer and Morris, 1995a, Storchak, Brewer and Morris, 1995b), liquid ((Storchak, Brewer and Morris, 1996c) and solid neon and argon (Storchak, Brewer and Morris (unpublished)) have shown that the spatial distribution of the ionisation track products is highly anisotropic with respect to the final position of the muon: the μ^+ thermalises well "downstream" from the end of its track. Some of the excess electrons generated in this track turn out to be mobile enough to reach the thermalised muon and form the hydrogen-like muonium (Mu $\equiv$ μ^+e^-) atom.

The phenomenon of *delayed* Mu formation (Percival, Roduner and Fischer 1978) described above is crucially dependent on electron interaction with the environment through its influence on *electron mobility*, namely whether an electron becomes a polaron or occupies the conduction band (in other words, whether electron is *localised* or *delocalised*) . In this chapter we consider several examples where μSR techniques allow one to distinguish between these two cases.

3.1 Solid nitrogen

Both muonium (Mu) and diamagnetic (D) signals are evident in solid N_2 at all temperatures (Storchak, Brewer and Morris, 1994b). Figure 12 shows the correlation between the muonium amplitude and the electron mobility in solid nitrogen: both have similar temperature dependences (Storchak, Brewer and Morris, 1994b).

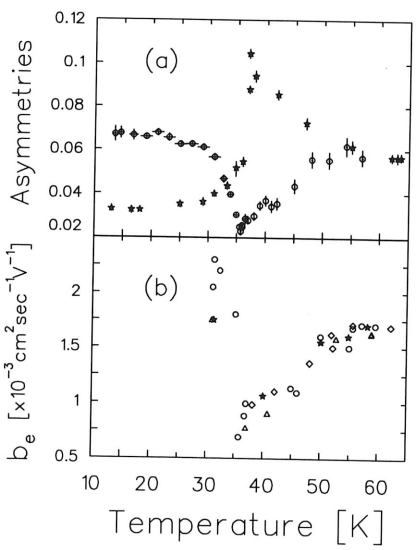

Figure 12. *(a) Temperature dependences of the muonium (circles) and diamagnetic μ^+ (stars) TF-μSR precession amplitudes (asymmetries) in solid nitrogen. (b) Temperature dependence of the electron mobility in solid nitrogen.*

The straightforward implication is that Mu formation in s-N_2 is at least partially due to convergence of the μ^+ and a radiolysis electron. In s-N_2 positive charges have been

found to be immobile (Loveland *et al.* 1972b), so the e^- must move to the μ^+.

Rather strong evidence in support of this picture comes from the electric field dependences of the diamagnetic and Mu amplitudes (Figure 13). A positive sign for E signifies that the electric field is applied in the same direction as the initial muon momentum. The results show that, on average, muons thermalise downstream from the last radiolysis electrons of the muon's ionisation track; in this case a positive E will pull the μ^+ and e^- apart, giving rise to an increased D amplitude, whereas a negative E will push the μ^+ and e^- together. The characteristic muon-electron distance R in solid α-N_2 was estimated from these measurements to be about $5{\times}10^{-6}$cm (Storchak, Brewer and Morris 1995a, Storchak, Brewer and Morris 1995b). Analogous measurements in β-N_2 at $T = 59$K revealed a much weaker electric field dependence, giving an estimate of the characteristic μ^+–e^- distance of about half that in α-N_2 (Storchak *et al.* 1998).

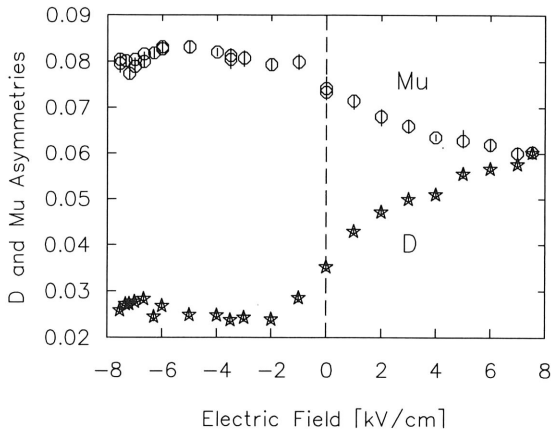

Figure 13. *Electric field dependences of muonium (Mu, circles) and diamagnetic (D, stars) amplitudes in α-N_2 at $T = 20K$.*

The characteristic time τ for e^- transport to the μ^+ can be determined by measurement of the *magnetic* field dependence of the Mu amplitude. Assuming that the muonium formation process is governed by a first-order kinetic equation $dn_{\rm Mu}(t) = -dn_\mu(t) = \lambda n_\mu(t)dt$, where $\lambda \equiv 1/\tau$ is the characteristic formation rate, the muonium amplitude has been shown (Percival, Roduner and Fischer 1978) to be

$$A_{\rm Mu} \propto \frac{\lambda}{\sqrt{\lambda^2 + \omega_{\rm Mu}^2}} \,. \tag{16}$$

For a weak local electric field E the electron mobility b_e is independent of E and the charge drift velocity v is defined by

$$v = b_e E. \tag{17}$$

In the absence of an applied field, the electric field at a distance r from the muon is $E = e/\epsilon r^2$, which can be integrated to give an expression for the Mu formation time

$$\tau = \frac{R^3 \epsilon}{3eb_e} \,. \tag{18}$$

Very near the muon, E is large and b_e is no longer constant; however, Equation (18) turns out to be a good approximation anyway because τ is determined mainly by slow motion at large distances in low electric fields. Equations (16) and (18) allow one to estimate the electron mobility b_e.

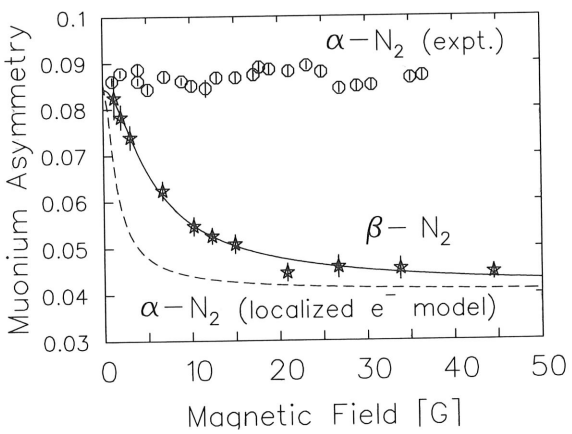

Figure 14. *Experimental magnetic field dependences of muonium amplitudes in α-N_2 at $T = 20K$ (circles) and in β-N_2 at $T = 59K$ (stars). Smooth curves represent numerical calculations in the framework of a localised electron model (see text).*

Figure 14 shows the magnetic field dependence of A_{Mu} in α-N_2 (circles) and in β-N_2 (stars). In β-N_2 the estimate of the electron mobility from μSR measurements using Equations (16) and (18) gives a value of the same order of magnitude as that extracted by time-of-flight (TOF) techniques. The dashed curve shows numerical calculations according to Equations (16) and (18) with the values of electron mobility determined from TOF measurements (Loveland 1972b) in α-N_2. The experiment, however, show that A_{Mu} is field independent (*i.e.* $\lambda \gg \omega_{\mathrm{Mu}}$), which means that the Mu formation time is much shorter than expected from TOF measurements. Using Equation (16) one can estimate a *lower* limit for the electron mobility in α-N_2: $b_e > 100\mathrm{cm}^2\,\mathrm{s}^{-1}\,\mathrm{V}^{-1}$ — a value *more* than 10^5 times higher than the electron mobility in β-N_2. The discrepancy between TOF and μSR results in α-N_2 is probably connected to crystal cracking at the α-β transition of s-N_2: The TOF technique (Loveland *et al.* 1972b), which relies on electron drift over the *macroscopic* distances between electrodes (typically about 10^{-2}cm), is inevitably sensitive to crystal imperfections. We claim that the μSR technique, which involves *microscopic* characteristic distances ($\sim 10^{-6}$ to 10^{-5}cm), avoids these difficulties.

Such a high electron mobility suggests that the electron transport mechanism in α-N_2 is fundamentally different from that in β-N_2. Probably the *localisation* of electrons *does not occur* in α-N_2 and Shockley's delocalised approximation (Shockley 1951) can be applied. A possible mechanism for electron localisation in β-N_2 may be interactions with the rotational modes of N_2 molecules — a scattering mechanism that is absent in α-N_2 due to the orientational ordering of the molecules.

3.2 Rare gas solids and liquids

Rare gas solids (RGS) and liquids (RGL) form a group of cryocrystals and cryoliquids characterised by very weak Van der Waals interatomic interactions. Early studies revealed charge transport in monatomic RGS (Miller *et al.* 1968, Spear and Le Comber 1977) to be fundamentally different from that in diatomic solids (Loveland 1972b). The remarkable transport properties of rare gas solids suggest that excess electrons occupy the conduction band. Therefore the phenomenon of electron *delocalisation* was invoked in order to describe electron transport in RGS.

The high value of the electron mobility leads to a breakdown of the proportionality between v and E [see Equation (17)] at a moderate electric field $E \gg u/b_e$ (Shockley 1951):

$$v = (32/3\pi)^{1/4}(b_e E u)^{1/2}, \tag{19}$$

where u is the velocity of sound. This result is obtained by evaluation of "hot" electron scattering on crystal excitations. Shockley's approach is based on the assumption that in a weakly scattered electronic system the electric field displaces the electronic energy distribution $\mathcal{D}(\varepsilon)$ toward higher energies while the shape of $\mathcal{D}(\varepsilon)$ remains Maxwellian. At low electric field the rate of energy gain by individual electrons from the applied field is equal to the rate of energy loss by scattering on lattice excitations and Equation (17) is valid. In high enough electric field in a system where "effective" lattice excitations are somehow suppressed (such as the freezing out of the orientational degrees of freedom in α-N_2 due to orientational ordering) this energy loss channel becomes ineffective and the electron subsystem is no longer in thermal equilibrium with the lattice; such "heating up" of the electron distribution causes a transition from Equation (17) to Equation (19). This characteristic transition from a linear E-dependence (17) to an $E^{1/2}$ dependence was observed experimentally in a number of insulators and semiconductors, for example in rare gas solids (Miller *et al.* 1968, Spear and Le Comber 1977) and in n-type Ge (Ryder and Shockley 1951). These measurements imply that in RGS electrons are no longer in thermal equilibrium with the lattice in electric fields as low as 100V/cm.

Experiments using TOF techniques clearly indicate that electron mobilities in heavy RGS (Ar, Kr and Xe) are of the same order of magnitude in solid and liquid phases (Spear and Le Comber 1977). The conductivity of many perfect metals and semiconductors exhibits this same feature, suggesting the existence of a band of extended electron states in *liquids* (including insulators). However, in the light RGL (He and Ne) the mobility of excess electrons was found to be some five orders of magnitude lower than in the heavy RGL (Meyer *et al.* 1962, Bruschi *et al.* 1972, Loveland *et al.* 1972a). Such a dramatic difference in electron mobility between light and heavy RGL has been interpreted (Spear and Le Comber 1977) as arising from electron *localisation* in a "bubble" in the former, contrasted with quasi-free propagation of *delocalised* electrons in the latter.

Such bubbles form because of the Pauli exclusion principle: a space is opened up around the excess electron by a strong short-range repulsive exchange interaction between it and the electrons of host atoms. Once the excess electron is thus localised, its zero-point kinetic energy tends to expand the resultant bubble, while weak long-range attractive interactions (caused by the polarisability of host atoms) tend to contract it, assisted by pressure-volume and surface energies. In liquid He the repulsive part of the interaction is strong while (due to a low polarisability) the attractive part is weak, leading to formation

of a stable bubble with a radius of about 10–20Å. Polarisability increases with increasing atomic number until in liquid Ar, Kr and Xe its attractive contribution overcomes the repulsive part of the interaction. Therefore electron localisation in a bubble *does not occur* in heavy RGL.

Liquid neon (ℓ-Ne) represents a borderline case where the total bubble energy turns out to be very close to that of a free electron. Early TOF experiments (1962, Bruschi *et al.* 1972, Loveland *et al.* 1972a) revealed only low mobility negative carriers in ℓ-Ne which were identified as stable electronic bubbles. However, μSR experiments (Storchak, Brewer and Morris 1996c) have found a *delocalised* electron state in ℓ-Ne.

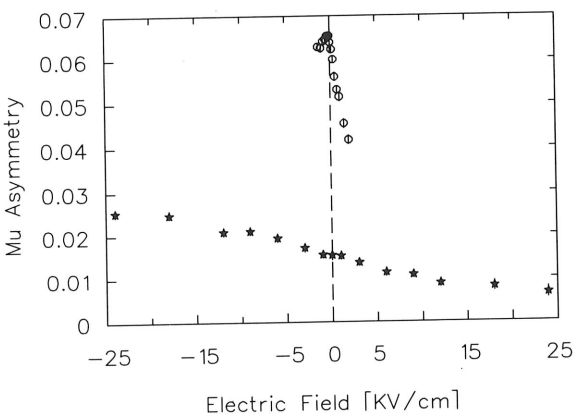

Figure 15. *Electric field dependences of the muonium amplitudes in solid Ne (circles) and liquid Ne (stars).*

Figure 15 presents the electric field dependences of the muonium amplitudes in solid and liquid Ne. If one assumes that *all* electrons in ℓ-Ne are *localised* in bubbles then these localised charges would move as *polarons* in low electric fields according to Equation (17). The low values for drift mobilities of localised charges in ℓ-Ne will inevitably cause loss of phase coherence among precessing Mu atoms formed at different times and the amplitude of the Mu precession signal will be drastically reduced. Since this is emphatically not the case, one must conclude that the muonium formation time is much less than that estimated in the framework of the *localised* charge transport model. This in turn implies a much higher electron mobility, consistent with Mu formation in ℓ-Ne due primarily to transport of *delocalised* electrons to positive muons.

4 Conclusions

Recent studies on both quantum diffusion of muonium atom and electron transport in condensed matter have demonstrated considerable power of muon spin relaxation techniques in determination of the quantum state of these particles. The dynamics of neutral and charged particles is basically governed by different mechanisms of *localisation* and *delocalisation*.

References

Anderson P W, 1958, *Phys. Rev.* **109** 1492.

Andreev A F and Lifshitz I M, 1969, *Sov.Phys.JETP* **29** 1107.

Brewer J H, 1995, Muon Spin Rotation/Relaxation/Resonance, *Encyclopedia of Applied Physics*, editor Trigg G L (VCH, New York, 1995).

Bruschi L, Mazzi G and Santini M, 1972, *Phys. Rev. Lett.* **28** 1504-1506.

Caldeira A O and Leggett A J, 1983a, *Phys. Rev. Lett.* **46,** 211.

Caldeira A O and Leggett A J, 1983b, *Ann. Phys. (N.Y.)* **149** 374.

Celio M, 1987, *Helv. Phys. Acta* **60** 600.

Cox S F J, 1987, *J. Phys. C* **20** 3187.

Cox S F J and Sivia D S, 1994, *Hyperfine Int.* **87** 971.

Flynn C P and Stoneham A M, 1970, *Phys. Rev. B* **1** 3966.

Grabert H and Weiss U, 1985, *Phys. Rev. Lett.* **54** 1065.

Guyer R A and Zane L I, 1969, *Phys.Rev.* **188** 445.

Hayano R S *et al.*, 1979, *Phys. Rev. B* **20** 850.

Holstein T, 1959 *Ann. Phys.* **8,** 343.

Kadono R, 1992, *Perspectives in Meson Science*, 113, editors Yamazaki T, Nakai K and Nagamine K (North-Holland, Amsterdam).

Kagan Yu and Klinger M I, 1976a, *Zh. Eksp. Teor. Fiz.* **70** 255.

Kagan Yu and Klinger M I, 1976b, [*Sov. Phys. JETP* **43** 132.

Kagan Yu M and Prokof'ev N V, 1990, *Phys. Lett. A* **150** 320 (1990) .

Yu M Kagan and Prokof'ev N V, 1992, Quantum Tunneling Diffusion in Solids, 37 *Quantum Tunneling in Condensed Media*, editors Leggett A J and Kagan Yu M (North-Holland.

Kadono R, 1990, *Hyperfine Int.* **64** 615.

Karlsson E *et al.*, 1995, *Phys. Rev. B* **52** 6417.

Kiefl R F *et al.*, 1981, *J. Chem. Phys.* **74** 308.

Kondo J, 1984a, *Physica B* **125** 279.

Kondo J, 1984b, *Physica B* **126** 377.

Krasnoperov E, Meilikhov E, Abela R, Herlach D, Morenzoni E, Gygax F, Shenck A, Eschenko D, 1992, *Phys. Rev. Lett.* **69** 1560–1563.

Kubo R, 1954, *J. Phys. Soc. Jpn.* **9** 935.

Kubo R and Toyabe T, 1966, *Magnetic Resonance and Relaxation*, 810, editor Blinc R (North-Holland, Amsterdam).

Lifshitz I M and Kagan Yu M, 1972a *Zh. Eksp. Teor. Fiz.* **62** 385.

Lifshitz I M and Kagan Yu M, 1972b *Sov. Phys. JETP* **35** 206.

Loveland R J *et al.*, 1972a, *Phys. Lett. A* **39** 225.

Loveland R J, Le Comber P G and Spear W E *et al.*, 1972b*Phys. Rev.B* **6** 3121–3127.

Luke G M, 1991, *et al.*, *Phys. Rev.* **43** 3284.

Meyer L *et al.*, 1962, *Phys. Rev.* **126** 1927.

Mikheev V A*et al.*, 1977, *Fiz. Nizk. Temp.* **3** 386.

Miller L S, Howe S and Spear W E, 1968, *Phys. Rev.* **166** 871–878.

Percival P W, Roduner E and Fischer H, 1978, *Chem. Phys.* **32** 353–367.

Prokof'ev N V, 1994, *Hyperfine Int.*, **85** 3.

Regelmann T, Schimmele L and Seeger A, 1995, *Phil. Mag. B* **72,** 209.

Richards M G *et al.*, 1976, *J. Low Temp.Phys.* **24** 1.

Ryder E J and Shockley W, 1951, *Phys. Rev.* **81** 139.

Schenck A, 1986, Muon Spin Rotation: Principles and Applications in Solid State Physics, (Adam Hilger, Bristol.)

Shockley W, 1951, *Bell System Tech. J.* **30** 900.

Slichter C P, 1980, *Principles of Magnetic Resonance* (Springer-Verlag).
Spear W E and Le Comber P G, 1977, Electronic transport properties, *Rare Gas Solids*, 1120, editors Klein M L and Venables J A, (Academic Press, New York).
Stamp P C E and Zhang Chao , 1991, *Phys. Rev. Lett.* **66** 1902.
Steinbinder D *et al.*, 1988, *Europhys. Lett.* **6** 535.
Storchak V *et al.*, 1992a, *Phys. Lett. A* **32** 77.
Storchak V *et al.*, 1992b, *Chem. Phys. Lett.* **200** 546.
Storchak V *et al.*, 1993, *Phys. Lett. A* **182** 449.
Storchak V G*et al.*, 1994, *Phys. Rev. Lett.* **72** 3056.
Storchak V *et al.*, 1995, *Phil. Mag. B* **72** 233.
Storchak V *et al.*, 1996, *Phys. Rev. B* **53** 662.
Storchak V, Brewer J H, and Morris G D, 1994a, *Hyperfine Int.* **85** 117.
Storchak V, Brewer J H and Morris G D, 1994b,*Phys. Lett. A* **193** 199–205.
Storchak V, Brewer J H and Morris G D, 1995a,*Phys. Rev. Lett.* **75** 2384–2387.
Storchak V, Brewer J H and Morris G D, 1995b,*Phil. Mag.* **72** 241–249.
Storchak V, Brewer J H, and Morris G D, 1996a, *Phys. Rev. B* **53** 11300.
Storchak V, Brewer J H, and Morris G D, 1996b, *Hyperfine Int.* **97–98** 323.
Storchak V, Brewer J H and Morris G D, 1996c, *Phys. Rev. Lett.*, **76** 2969–2972.
Storchak V, Brewer J H, and Morris G D,Arseneau A J and Senba M, 1998, *Phys. Rev. B* (in press).
Storchak V G, Eschenko D G, Brewer J H, Cottrell S P and Cox S F J, (unpublished).
Storchak V G and Prokof'ev N V, 1998 *Rev. Mod. Phys.* **70** 929.
Verkin B I and Prikhotko A F (editors), 1983, *Cryocrystals*, (Kiev).
Waite T R, 1957, *Phys. Rev.* **107** 463.
Weiss U, 1993, Quantum Dissipative Systems, *Series in Modern Condensed Matter Physics*, vol.2, (World Scientific, Singapore.
Weiss U and Grabert H, 1985, *Phys. Lett. A* **108,** 63.
Yamada K, 1984, *Prog. Theor. Phys.* **72** 195.
Yen H K, 1988, M.Sc. thesis, University of British Columbia (unpublished).